Free-vibration analysis of a three-dimensional soil–structure system

J. L. Wegner[1] and Xiong Zhang[2,*,†]

[1]*Department of Mechanical Engineering, University of Victoria, PO Box 3055, Victoria, B.C., Canada V8W 3P6*
[2]*Department of Engineering Mechanics, Tsinghua University, Beijing 100084, P.R. China*

SUMMARY

A procedure which involves a non-linear eigenvalue problem and is based on the substructure method is proposed for the free-vibration analysis of a soil–structure system. In this procedure, the structure is modelled by the standard finite element method, while the unbounded soil is modelled by the scaled boundary finite element method. The fundamental frequency, and the corresponding radiation damping ratio as well as the modal shape are obtained by using inverse iteration. The free vibration of a dam–foundation system, a hemispherical cavity and a hemispherical deposit are analysed in detail. The numerical results are compared with available results and are also verified by the Fourier transform of the impulsive response calculated in the time domain by the three-dimensional soil–structure–wave interaction analysis procedure proposed in our previous paper. The fundamental frequency obtained by the present procedure is very close to that obtained by Touhei and Ohmachi, but the damping ratio and the imaginary part of modal shape are significantly different due to the different definition of damping ratio. This study shows that although the classical mode-superposition method is not applicable to a soil–structure system due to the frequency dependence of the radiation damping, it is still of interest in earthquake engineering to evaluate the fundamental frequency and the corresponding radiation damping ratio of the soil–structure system. Copyright © 2001 John Wiley & Sons, Ltd.

KEY WORDS: soil–structure interaction; coupling method; non-linear eigenvalue problem; earthquake engineering; numerical method

1. INTRODUCTION

The dynamic interactions at soil–structure interfaces play an important role in the seismic response of structures. These interactions cause energy dissipation, and change the natural modes of vibration of the structure such as natural frequencies and the corresponding mode shapes. This has motivated many numerical studies to evaluate these interactions. Based on the direct method, many kinds of transmitting boundaries [1, 2] have been developed over the past two decades to satisfy the radiation condition. Many hybrid methods (coupling methods) [3–5]

---

have also been developed based on the substructure method, where the structure and an adjacent finite region of soil are modelled by the standard finite element method, while the unbounded soil is modelled by the boundary element method or the scaled boundary finite element method [7], which is otherwise called the consistent infinitesimal finite element cell method [8]. Most of these studies are mainly concerned with the energy dissipation caused by dynamic interactions. However, for a close investigation of the interaction effects on a structure–soil system, it is desirable to evaluate the free-vibration frequencies, especially the few low-frequency modes of vibrations. Touhei and Ohmachi proposed a modal analysis procedure [6] based on an FE–BE method in the time domain along with the classical mode-superposition method and applied it to a dam–foundation system. In their procedure, the eigenvalues are evaluated from the poles of the frequency response function, which is calculated by the FE–BE method.

Because the dynamic-stiffness matrix is frequency dependent and complex, the orthogonality condition is not satisfied for a soil–structure system. Consequently, the equations of motion cannot be uncoupled, and the classical mode-superposition method is not applicable to the soil–structure system. However, it is still of interest in earthquake engineering to investigate the free-vibration frequencies and the corresponding radiation damping ratios, especially for the modes of vibration with the lowest frequencies.

In the substructure method, the effect of the unbounded soil on the structure is represented by a force–displacement relationship. Based on the substructure method, a non-linear eigenvalue problem is obtained in this paper for the analysis of the free vibration of a three-dimensional soil–structure system. The scaled boundary finite element method is then used to model the unbounded soil, while the finite element method is used to model the structure. Inverse iteration is used to solve the non-linear eigenvalue problem. The fundamental frequency and the corresponding radiation damping ratio as well as the eigenvector are obtained. The free vibration of a dam–foundation system, a cavity and a deposit are analysed in detail. The results obtained by this method are also verified by using the Fourier transform of the impulsive response of a soil–structure system calculated by the three-dimensional soil–structure–wave interaction analysis procedure proposed in Reference [5].

2. BASIC EQUATION

2.1. Equations of motion

For a soil–structure system without applied force, the equations of motion of the structure in the frequency domain can be expressed as [9]

$$\begin{bmatrix} \mathbf{S}_{ss}(\omega) & \mathbf{S}_{sb}(\omega) \\ \mathbf{S}_{bs}(\omega) & \mathbf{S}_{bb}(\omega) \end{bmatrix} \begin{Bmatrix} \mathbf{u}_s^{\mathrm{t}}(\omega) \\ \mathbf{u}_b^{\mathrm{t}}(\omega) \end{Bmatrix} = \begin{Bmatrix} 0 \\ -\mathbf{r}_b(\omega) \end{Bmatrix} \tag{1}$$

where the dynamic stiffness matrix $\mathbf{S}$ of the structure is calculated as

$$\mathbf{S}(\omega) = \mathbf{K}(1 + 2\xi_h \mathrm{i}) - \omega^2 \mathbf{M} \tag{2}$$

in which ξ_h is the damping ratio, $\mathbf{M}$ is the mass matrix, $\mathbf{C}$ is the viscous damping matrix, $\mathbf{K}$ is the stiffness matrix of the structure, $\mathbf{u}(\omega)$ is the displacement vector, and $\mathbf{r}_b(\omega)$ is the ground interaction force. In (1), the subscripts b, and s denote the nodes on the soil–structure
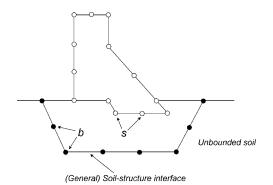
Figure 1. Soil–structure system.

interface, and the remaining nodes of the structure, respectively, as shown in Figure 1, and the superscript t denotes the total motion of the structure.

2.2. Ground interaction force

The ground interaction forces, $\mathbf{r}_b(\omega)$, play an important role in the free vibration of a soil–structure system because they represent the effects of the unbounded soil on the structure. It makes the equations of motion (1) for free vibration of a soil–structure system more difficult to solve. The ground interaction forces $\mathbf{r}_b(\omega)$ are given by

$$\mathbf{r}_b(\omega) = \bar{\mathbf{S}}_{bb}^{g}(\omega)(\mathbf{u}_b^{t}(\omega) - \mathbf{u}_b^{g}(\omega)) \tag{3}$$

where the superscript g denotes the unbounded soil with excavation, $\mathbf{u}_b^{g}(\omega)$ is the displacement at the nodes b (which subsequently lie on the structure–soil interface) of the ground with excavation, and $\bar{\mathbf{S}}_{bb}^{g}(t)$ is the dynamic stiffness matrix of the ground with excavation which is calculated by the scaled boundary finite element method in the frequency domain [8].

For free vibrations of the soil–structure system, the scattered motion of incident waves, $\mathbf{u}_b^{g}(\omega) = 0$.

2.3. Non-linear eigenvalue problem

Substituting Equation (3) into Equation (1) results in

$$\left((1 + 2\xi_h \mathrm{i}) \begin{bmatrix} \mathbf{K}_{ss} & \mathbf{K}_{sb} \\ \mathbf{K}_{bs} & \mathbf{K}_{bb} + \frac{\bar{\mathbf{S}}_{bb}^{g}(\omega)}{(1+2\xi_h \mathrm{i})} \end{bmatrix} - \omega^2 \begin{bmatrix} \mathbf{M}_{ss} & \mathbf{M}_{sb} \\ \mathbf{M}_{bs} & \mathbf{M}_{bb} \end{bmatrix} \right) \begin{Bmatrix} \mathbf{u}_s^{t} \\ \mathbf{u}_b^{t} \end{Bmatrix} = 0 \tag{4}$$

Equation (4) is a non-linear eigenvalue problem. The dynamic-stiffness matrix is a frequency-dependent complex matrix, hence Equation (4) is more difficult to solve. There are several methods to solve this non-linear eigenvalue problem, such as the inverse iteration method [10], Newton's method [11], and Jacobi–Davidson iterations method [12].

The free-vibration frequencies and the corresponding modal shapes can be obtained as the solution of Equation (4), but the orthogonality condition is not satisfied for the soil–structure

system, consequently the modal shapes cannot be used to uncouple the equations of motion to solve them efficiently. However, the free-vibration frequencies and the corresponding radiation damping ratios of the lowest few modes of vibration are still of interest in earthquake engineering. It is possible to obtain all free-vibration frequencies and the corresponding mode shapes, but the fundamental frequency of a soil–structure system is the most important in earthquake engineering. The inverse iteration is used in this paper to evaluate the fundamental frequency, the corresponding radiation damping ratio and the mode shape efficiently from Equation (4).

For the case in which no structure exists, Equation (4) cannot be solved directly. To overcome this difficulty, the complex dynamic-stiffness matrix $\bar{\mathbf{S}}_{bb}^{\mathrm{g}}(\omega)$ is decomposed as

$$\bar{\mathbf{S}}_{bb}^{\mathrm{g}}(\omega) = \bar{\mathbf{K}}_{bb}^{\mathrm{g}} + \bar{\mathbf{S}}_{bb}^{\mathrm{g}1}(\omega) \tag{5}$$

where the matrix $\bar{\mathbf{K}}_{bb}^{\mathrm{g}} = \bar{\mathbf{S}}_{bb}^{\mathrm{g}}(0)$ is a real matrix, which represents the static stiffness matrix of the unbounded soil. Substituting Equation (5) into Equation (4) leads to

$$[(1 + 2\xi_h \mathrm{i})\mathbf{K} - \omega^2 \bar{\mathbf{M}}(\omega)]\mathbf{u}^{\mathrm{t}} = 0 \tag{6}$$

where

$$\mathbf{K} = \begin{bmatrix} \mathbf{K}_{ss} & \mathbf{K}_{sb} \\ \mathbf{K}_{bs} & \mathbf{K}_{bb} + \dfrac{\bar{\mathbf{K}}_{bb}^{\mathrm{g}}}{(1+2\xi_h \mathrm{i})} \end{bmatrix}$$

$$\bar{\mathbf{M}}(\omega) = \begin{bmatrix} \mathbf{M}_{ss} & \mathbf{M}_{sb} \\ \mathbf{M}_{bs} & \mathbf{M}_{bb} + \bar{\mathbf{M}}_{bb}^{\mathrm{g}1}(\omega) \end{bmatrix}$$

$$\bar{\mathbf{M}}_{bb}^{\mathrm{g}1}(\omega) = \begin{cases} -\dfrac{\bar{\mathbf{S}}_{bb}^{\mathrm{g}}(\omega) - \bar{\mathbf{K}}_{bb}^{\mathrm{g}}}{\omega^2} & \text{for } \omega > 0 \\ 0 & \text{for } \omega = 0 \end{cases}$$

The inverse iteration solution of Equation (6) is formulated by

$$\mathbf{u}^{\mathrm{t}(0)} = [1, 1, \dots, 1]^{\mathrm{T}}$$

$$\mathbf{K}\bar{\mathbf{u}}^{\mathrm{t}(j)} = \bar{\mathbf{M}}(\omega^{(j-1)})\mathbf{u}^{\mathrm{t}(j-1)}$$

$$\mathbf{u}^{\mathrm{t}(j)} = \frac{\bar{\mathbf{u}}^{\mathrm{t}(j)}}{\max(\bar{\mathbf{u}}^{\mathrm{t}(j)})} \tag{7}$$

$$\lambda^{(j)} = \frac{(\bar{\mathbf{u}}^{\mathrm{t}(j)})^{\mathrm{T}}\bar{\mathbf{M}}(\omega^{(j-1)})\mathbf{u}^{\mathrm{t}(j-1)}}{(\bar{\mathbf{u}}^{\mathrm{t}(j)})^{\mathrm{T}}\bar{\mathbf{M}}(\omega^{(j-1)})\bar{\mathbf{u}}^{\mathrm{t}(j)}}$$

$$\omega^{(j)} = \sqrt{\lambda^{(j)}(1 + 2\xi_h \mathrm{i})}$$

where $\max(\bar{\mathbf{u}}^{\mathrm{t}(j)})$ is the largest element of the $\bar{\mathbf{u}}^{\mathrm{t}(j)}$ which is used to normalize the $\bar{\mathbf{u}}^{\mathrm{t}(j)}$. In Equation (7), the matrix $\mathbf{K}$ is a complex constant matrix, therefore it is factored only once throughout the iterations. From Equation (7), the fundamental frequency, the corresponding radiation damping ratio and mode shape can be obtained. The free-vibration frequency of the

jth mode of vibration obtained from Equation (7) or Equation (4) can be expressed in the following form:

$$\omega_j = a_j + \mathrm{i}b_j \tag{8}$$

where a_j and b_j are the real and imaginary parts of ω_j. The free-vibration motion of the jth mode can be written as

$$\mathbf{u}_j^{\mathrm{t}}(t) = \mathbf{u}_j^{\mathrm{t}} \exp(-b_j t + \mathrm{i}a_j t) \tag{9}$$

Equation (9) represents the free vibration of a damped system. The free-vibration frequency of the damped system of the jth mode of vibration, ω_{D_j}, and the corresponding damping ratio, ξ_j, can be obtained as

$$\omega_{\mathrm{D}_j} = a_j \tag{10}$$

$$\xi_j = \frac{b_j}{\sqrt{a_j^2 + b_j^2}} \tag{11}$$

respectively.

If the hysteretic damping ratio of a structure, ξ_h, is equal to zero, the damping ratio ξ_j obtained from Equation (11) is the radiation damping ratio. Otherwise, the effect of hysteretic damping is included in the damping ratio ξ_j. Consider any two positive peaks which are m cycles apart, such as u_j^n and u_j^{n+m} which occur at times $n(2\pi/a_j)$ and $(n+m)2\pi/a_j$, respectively. Using Equation (9), the ratio of these two values is given by

$$u_j^n / u_j^{n+m} = \exp(2\pi m b_j / a_j) \tag{12}$$

The damping ratio, ξ_j, follows from Equations (11) and (12) as

$$\xi_j = \frac{\delta}{\sqrt{4\pi^2 m^2 + \delta^2}} \tag{13}$$

where $\delta = \ln u_j^n / u_j^{n+m}$.

3. ANALYTICAL EXAMPLE

3.1. Spherical cavity embedded in full-space

The free vibration in radial direction of a spherical cavity embedded in full space is analysed. The dynamic-stiffness matrix is given by [8]

$$\bar{S}_{bb}^g(a_0) = K^\infty \left(1 - \frac{\beta a_0^2}{1 + a_0^2} + \mathrm{i}a_0 \frac{\beta a_0^2}{1 + a_0^2} \right) \tag{14}$$

where the non-dimensional frequency $a_0 = \omega r_0 / c_{\mathrm{p}}$, the static-stiffness coefficient $K^\infty = 16\pi G r_0$, $\beta = (1 - v)/2(1 - 2v)$, r_0 is the radius of the cavity, c_{p} is the dilatational wave velocity, G is the shear modulus, and v is Poisson's ratio.

In this case, no structure exists, that is $\mathbf{K}_{ss} = \mathbf{K}_{sb} = \mathbf{M}_{ss} = \mathbf{M}_{sb} = \mathbf{C}_{ss} = \mathbf{C}_{sb} = 0$ in Equation (4). Substituting Equation (14) into Equation (4) leads to

$$K^{\infty} \left(1 - \frac{\beta a_0^2}{1 + a_0^2} + \mathrm{i} a_0 \frac{\beta a_0^2}{1 + a_0^2} \right) U_b^{\mathrm{t}} = 0 \tag{15}$$

Solving Equation (15) for the non-dimensional frequency, a_0, gives

$$a_0 = \frac{1}{2\beta} (\mathrm{i} \pm \sqrt{4\beta - 1}) \tag{16}$$

The radiation damping ratio ξ and the free-vibration frequency ω_{D} of the spherical cavity are given by

$$\omega_{\mathrm{D}} = \frac{c_s}{r_0} \sqrt{\frac{2}{1 - v}} \tag{17}$$

$$\xi = \sqrt{\frac{1 - 2v}{2(1 - v)}} \tag{18}$$

Equations (17) and (18) show that the free-vibration frequency of the spherical cavity embedded in full space in the radial direction varies between $\sqrt{2} c_s / r_0$ and $2c_s / r_0$, while the radiation damping ratio varies between 0 and $\sqrt{2}/2$. The radiation damping ratio only depends on Poisson's ratio. The ratio of two successive positive peaks follows from Equations (12) and (16)

$$u_n / u_{n+1} = \exp \left(\frac{2\pi}{\sqrt{4\beta - 1}} \right) \tag{19}$$

To verify the free-vibration frequency and the radiation damping ratio given by Equations (17) and (18), the impulsive response of the cavity is analysed in the time domain. The following pressure pulse

$$p(t) = \begin{cases} \dfrac{p_0}{2} \left(1 - \cos \dfrac{2\pi t}{t_0} \right), & 0 \leqslant t \leqslant t_0 \\ 0, & t > t_0 \end{cases} \tag{20}$$

is applied uniformly to the wall of the cavity in the radial direction, where $t_0 = 3.46 \, r_0 / c_p$. The Poisson's ratio v is assumed to be 0.495. In the non-dimensional displacement response of the cavity to the pressure pulse as shown in Figure 2, the second positive peak $u_2 = 0.1605$ occurs at time $\tau = 39.878$ while the third positive peak $u_3 = 0.0856$ occurs at time $\tau = 71.628$. The free-vibration frequency and the damping ratio can be obtained from the impulsive response of the cavity as $\omega_{\mathrm{D}} r_0 / c_s = 1.989$ and $\xi = 0.0995$, which are the same as those calculated by Equations (17) and (18).
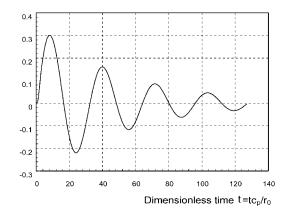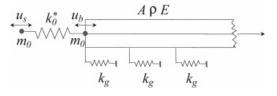
Figure 2. Displacement response.

Figure 3. A mass–spring system connected to a semi-infinite rod on elastic foundation.

3.2. Mass–spring system connected to a semi-infinite rod on elastic foundation

To illustrate the effect of unbounded soil on the free vibration of a structure in a soil–structure system, the free vibration of a mass–spring system, which is connected to a semi-infinite rod on an elastic foundation as shown in Figure 3, is studied.

In this spring–mass system, hysteretic damping is included by introducing the complex stiffness coefficient $k_0^* = k_0(1 + 2\xi_h i)$, where ξ_h is the damping ratio and k_0 is the stiffness coefficient of the spring. In Figure 3, the area of the cross-section of the semi-infinite rod is denoted by A, the mass density by ρ, the modulus of elasticity by E, and the static spring stiffness per unit length of the elastic foundation by k_g. The dynamic stiffness coefficient, $\bar{S}_{bb}^{g}(\omega)$, of the semi-infinite rod on an elastic foundation is given by [8]

$$\bar{S}_{bb}^{g}(\omega) = K^\infty \sqrt{1 - a_0^2} \tag{21}$$

where the static-stiffness coefficient $K^\infty = \sqrt{EAk_g}$, and the non-dimensional frequency $a_0 = \omega\sqrt{A\rho/k_g}$.

The dynamic-stiffness matrix of the semi-infinite rod on elastic foundation is a complex matrix, which is equivalent to a frequency-dependent spring and a frequency-dependent damper. Consequently, the mass–spring system connected to a semi-infinite rod on elastic foundation is equivalent to the system shown in Figure 4.
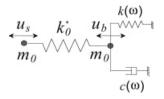
Figure 4. Equivalent system.

Substituting Equation (21) into Equation (4) results in

$$\begin{bmatrix} \omega_0^2 - \omega^2 & -\omega_0^2 \\ -\omega_0^2 & \omega_0^2 - \omega^2 + \dfrac{K^\infty}{m_0}\sqrt{1-a_0^2} \end{bmatrix} \begin{pmatrix} U_s \\ U_b \end{pmatrix} = 0 \qquad (22)$$

where $\omega_0^2 = (1 + 2\xi_h i)k_0/m_0$.

Assume the dimensionless material quantities to be $k_0/m_0 = 1$, $K^\infty/m_0 = 1$, $A\rho/k_g = 1$. Solving Equation (22) results in

$$\omega_1 = 0.57354, \qquad \omega_2 = 1.3455 + 0.1491i$$
$$\begin{pmatrix} U_s \\ U_b \end{pmatrix}_1 = \begin{pmatrix} 1 \\ 0.6711 \end{pmatrix} U, \qquad \begin{pmatrix} U_s \\ U_b \end{pmatrix}_2 = \begin{pmatrix} 1 \\ -0.7882 - 0.4014i \end{pmatrix} U$$

for $\xi_h = 0$, and

$$\omega_1 = 0.58128 + 0.01887i, \qquad \omega_2 = 1.33191 + 0.44645i$$
$$\begin{pmatrix} U_s \\ U_b \end{pmatrix}_1 = \begin{pmatrix} 1 \\ 0.7015 + 0.0975i \end{pmatrix} U, \qquad \begin{pmatrix} U_s \\ U_b \end{pmatrix}_2 = \begin{pmatrix} 1 \\ -0.7666 - 0.4666i \end{pmatrix} U$$

for $\xi_h = 0.2$, where U is a complex constant which is determined by the initial conditions. The free-vibration frequencies and the damping ratios of the system are obtained as

$$\omega_{D1} = 0.5735, \quad \xi_1 = 0$$
$$\omega_{D2} = 1.3455, \quad \xi_2 = 0.11$$

for $\xi_h = 0$, and

$$\omega_{D1} = 0.5813, \quad \xi_1 = 0.03$$
$$\omega_{D2} = 1.3319, \quad \xi_2 = 0.32$$

for $\xi_h = 0.2$. If the semi-infinite rod does not exist, e.g. $\mathbf{S}_{bb}^g(\omega) = 0$, the free-vibration frequencies and the corresponding modal shapes of the mass–spring system for $\xi_h = 0$ are

$$\omega_1 = 0, \quad \omega_2 = \sqrt{2}$$
$$\begin{pmatrix} U_s \\ U_b \end{pmatrix}_1 = \begin{pmatrix} 1 \\ 1 \end{pmatrix} U, \qquad \begin{pmatrix} U_s \\ U_b \end{pmatrix}_2 = \begin{pmatrix} 1 \\ -1 \end{pmatrix} U$$

Comparison of the free-vibration frequencies and modal shapes of the two systems shows that the unbounded soil not only affects the free-vibration frequencies, but also the modal shapes and phase angles. The frequencies and radiation damping ratios for different vibration modes can be obtained from Equations (10) and (11).

4. NUMERICAL STUDIES

4.1. Free vibration of a dam–foundation system

Touhei and Ohmachi evaluated the natural modes of vibration of a dam–foundation system shown in Figure 5 from the impulsive response calculated by the FE–BE method [6]. In their study, it is assumed that the impulsive response of the dam–foundation system calculated by the FE–BE method can be approximately represented by the classical mode superposition, so that the equations of motion can be decoupled. Based on this assumption, the free-vibration frequencies, equivalent damping ratios and mode shapes of the system are obtained.

To compare our results with available results, the same dam–foundation system is analysed by the present method. The model is made up of a triangular elastic homogeneous earthdam and an elastic homogeneous semi-infinite foundation. The deformation is assumed to be plane strain. The dam is modelled by the finite element method, while the foundation is modelled by the scaled boundary finite element method as shown in Figure 6. In this model, the soil adjacent to the dam is treated as a part of the structure, and the surface of the soil is treated as the soil–structure interface. Six cases are analysed, as shown in Table I. In Table I, the impedance ratio is defined as the ratio of the shear wave velocity of the dam to the shear wave velocity of the foundation since the density of the dam is assumed to equal the density of the foundation. Poisson's ratio is assumed to be 0.3 for both the dam and the foundation in all cases. The fundamental frequency and the corresponding radiation damping ratio are compared with those of Touhei and Ohmachi in Table II. The hysteretic damping ratio of the dam is taken as 0.0, 0.1, 0.2, and 0.3, respectively. The corresponding modal shape is shown in Figure 7 for $\xi_h = 0$, for case 4. The real part of the vibration shape is very close to that of Touhei and Ohmachi, but the imaginary part is different.

The fundamental frequencies obtained by the present method are very close to those obtained by Touhei and Ohmachi, but the damping ratios are significantly different. Actually, the damping ratios obtained by Touhei and Ohmachi are the equivalent damping ratios, instead of the radiation damping ratios. The equations of motion of the dam–foundation system can be decoupled by introducing these equivalent damping ratios. The damping ratios obtained in the present method are the true radiation damping ratios if ξ_h is equal to zero, which are obtained directly from the equations of motion of free vibration of the dam–foundation system and cannot be used to decouple the equations of the motion of the system. Hence, the damping ratios and the imaginary part of mode shapes obtained in the present method are different from those obtained by Touhei and Ohmachi.

To verify the results obtained by the present method, the force pulse,

$$P = \left(1 - \cos \frac{2\pi}{T}t\right), \quad t \leqslant T \tag{23}$$

Figure 5. A dam–foundation system.

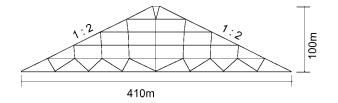Figure 6. Finite element model of the dam–foundation system.

Table I. Case analysis.

| | Shear wave velocity c_s (m/s) | | Impedance |
	Dam	Foundation	ratio
Case 1	300	1000	0.3
Case 2		2000	0.15
Case 3		3000	0.10
Case 4	500	1000	0.50
Case 5		2000	0.25
Case 6		3000	0.17

where T is the duration of the pulse, is applied at the top of the dam for case 4 (impedance ratio equals 0.5). An analysis is performed for two values of the duration T, namely, 0.6 s, and 0.05 s. Figure 8 shows the displacement responses at the top of the dam to the force pulses (23) and the amplitudes of their Fourier transform. For the force pulse with duration $T = 0.6$ s, only the first mode of vibration is excited, while for the force pulse with duration $T = 0.05$ s, many modes of vibration are excited. The fundamental frequency and the corresponding radiation damping ratio calculated from Figure 8(a) are 1.633 and 1.03 per cent, which are very close to those obtained by the present method.

To study the effect of the unbounded soil on the free vibration of a dam, the free vibration of the same dam laid on a rigid foundation is analysed. The fundamental frequencies and the corresponding damping ratios for the six cases are listed in Table III.

A comparison of Tables II and III shows that the fundamental frequency and the corresponding damping ratio of the dam–foundation system are very close to those of the same dam laid on a rigid foundation when the impedance ratio of the dam–foundation system

Table II. Fundamental frequencies and radiation damping ratios.

ξ_h		Impedance ratio					
		0.3	0.15	0.10	0.5	0.25	0.17
0.0	Freq. (Hz)	1.01(0.94*)	1.02(0.99)	1.03(1.00)	1.64(1.43)	1.69(1.57)	1.70(1.63)
	Damp (%)	0.25(10.6)	0.03(4.0)	0.004(2.8)	1.03(23.1)	0.12(7.5)	0.02(3.5)
0.1	Freq. (Hz)	1.02	1.03	1.03	1.64	1.70	1.71
	Damp (%)	9.83	9.81	9.83	10.18	9.80	9.79
0.2	Freq. (Hz)	1.03	1.04	1.05	1.66	1.73	1.74
	Damp (%)	18.63	18.81	18.85	18.56	18.68	18.76
0.3	Freq. (Hz)	1.05	1.07	1.07	1.70	1.76	1.77
	Damp (%)	26.17	26.53	26.61	25.72	26.30	26.47

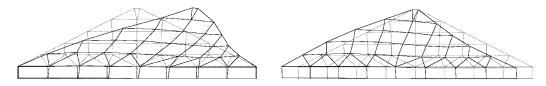* The results listed within a pair of brackets are those obtained by Touhei and Ohmachi.

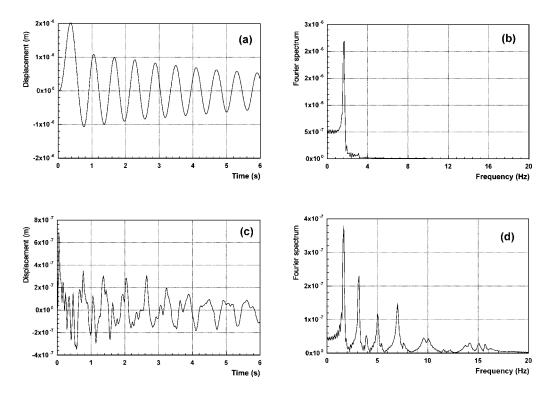Figure 7. Vibration shapes for $\xi_h = 0$, for case 4.

Figure 8. Displacement response at the top of the dam to the force pulse for case 4. In (a) and (b), the duration of the pulse equals 0.6 s, while in (c) and (d), the duration of the pulse equals 0.05 s.

is less than 0.3. However, due to the effect of the radiation damping of the non-rigid foundation, the response of these two systems to the same applied load is quite different, as shown in Figure 9.

4.2. Free vibration of a hemispherical cavity

The fundamental frequency and the corresponding radiation damping ratio of a hemispherical cavity are studied. In this case, only the surface of the cavity is discretized. The surface of the cavity is modelled by 12 eight-node two-dimensional isoparametric elements. Figure 10 illustrates the front view of the finite element mesh. The Poisson's ratio is assumed to be 0.25,

Table III. Fundamental frequencies and the corresponding damping ratios
of the dam laid on a rigid foundation.

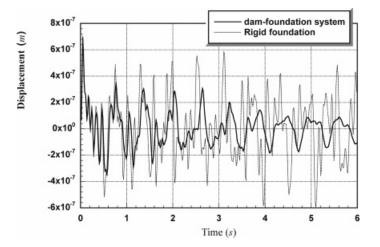| c_s (m/s)		Hysteretic damping ratio ξ_h					
		0.0	0.1	0.2	0.3	0.4	0.5
300	Freq. (Hz)	1.03	1.03	1.05	1.07	1.10	1.13
	Damp (%)	0.0	9.85	18.91	26.69	33.10	38.27
500	Freq. (Hz)	1.71	1.72	1.75	1.78	1.83	1.88
	Damp (%)	0.0	9.85	18.91	26.69	33.10	38.27

Figure 9. Displacement response at the top of the dam to the pulse force for case 4. The duration of
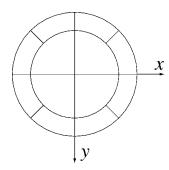the pulse force equals 0.5 s.

Figure 10. The front of view of the finite element mesh for the hemispherical cavity.

and the non-dimensional frequency, η_p, is defined as
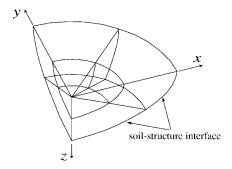
$$\eta_p = \frac{\omega R}{\pi c_p}$$

Figure 11. A quarter of the finite element mesh for the hemispherical deposit.

where R is the radius of the cavity, c_p is the dilatational wave velocity in half-space, ω is the circular frequency. The non-dimensional fundamental frequency and the corresponding radiation damping ratio are obtained as

$$\eta_{pD} = 0.097$$
$$\xi = 0.686$$

Wave scattering by the same hemispherical cavity was studied in the time domain in Reference [5], in which the numerical studies show that the numerical results are in good agreement with those obtained by the wave function expansion method for incident waves with low frequencies, say $\eta_p \leqslant 0.5$, which equals about 5 times the fundamental frequency of the cavity. Hence, this restriction on frequency does not prevent the application of the procedure proposed in Reference [5] in earthquake engineering problems.

4.3. Free vibration of a hemispherical deposit

Material properties for the deposit R and the half-space E are assumed to be related by $G^R = 0.3 G^E$ and $\rho^R = 0.6 \rho^E$, where G is the shear modulus and ρ is the density, with Poisson's ratio $v^R = 0.3$ and $v^E = 0.25$, respectively. The soil–structure interface is modelled by 12 eight-node two-dimensional isoparametric elements, while the deposit is modelled by 24 twenty-node three-dimensional isoparametric elements. Figure 11 illustrates a quarter of the finite element mesh. The non-dimensional fundamental frequency and the corresponding radiation damping ratio are obtained as

$$\eta_{pD} = 0.105$$
$$\xi = 0.653$$

The wave scattering by the same deposit was analysed numerically in Reference [5], for the non-dimensional frequency $\eta_p = 0.5$. The ratio of the non-dimensional frequency, η_p, to the non-dimensional fundamental frequency, η_{pD}, is less than 5, hence the numerical results obtained in Reference [5] are in good agreement with analytical results.

5. CONCLUDING REMARKS

Owing to the frequency dependence of the radiation damping, the orthogonality condition for the modes is not satisfied for a soil–structure system, hence the classic mode-superposition method is not applicable to the soil–structure system. However, it is still of interest in earthquake engineering to evaluate the fundamental frequency, and the corresponding radiation damping ratio.

The fundamental frequency obtained in this paper is very close to that obtained by Touhei and Ohmachi, but the corresponding damping ratio and the imaginary part of modal shape are significantly different. This is due to the different definition of the damping ratio. The damping ratio obtained by Touhei and Ohmachi is an equivalent damping ratio, which can be used to decouple the equations of motion of the dam–foundation system. However, the damping ratio obtained in the present paper is the actual radiation damping ratio, which is obtained by solving the non-linear eigenvalue problem.

The procedure proposed in this paper can be used to evaluate efficiently the fundamental frequency, and the corresponding radiation damping ratio as well as the modal shape. It is easy to extend the present procedure to obtain all free-vibration frequencies and the corresponding radiation damping ratios as well as modal shapes by employing a scheme, such as Newton's method, to solve the non-linear eigenvalue problem.

REFERENCES

1. Lysmer J, Kuhlemeyer RL. Finite dynamic model for infinite media. *Journal of Engineering Mechanics Division ASCE* 1969; **95**: 859–877.
2. Smith WD. A nonreflecting plane boundary for wave propagation problems. *Journal of Computational Physics* 1974; **15**: 492–503.
3. Zienkiewicz OC, Kelly DW, Betters P. The coupling of the finite element methods and boundary solution procedures. *International Journal for Numerical Methods in Engineering* 1977; **11**: 355–375.
4. Von Estorff O, Kausel E. Coupling of boundary and finite elements for soil–structure interaction problems. *Earthquake Engineering and Structural Dynamics* 1989; **18**: 1065–1075.
5. Zhang X, Wegner JL, Haddow JB. Three dimensional linear soil–structure–wave interaction analysis in time domain. *Earthquake Engineering and Structural Dynamics* 1999; **28**: 1501–1524.
6. Touhei T, Ohmachi T. Modal analysis of a dam–foundation system based on an FE–BE method in the time domain. *Earthquake Engineering and Structural Dynamics* 1994; **23**: 1–15.
7. Song Ch, Wolf JP. The scaled boundary finite-element method-alias consistent infinitesimal finite-element cell method — for elastodynamics. *Computer Methods in Applied Mechanics and Engineering* 1997; **147**: 329–355.
8. Wolf JP, Song C. *Finite-Element Modelling of Unbounded Media*. Wiley: New York, 1996.
9. Wolf JP. *Dynamic Soil–Structure-Interaction Analysis*. Prentice-Hall: Englewood Cliffs, NJ, 1985.
10. Ruhe A. Algorithms for the nonlinear eigenvalue problem. *SIAM Journal on Numerical Analysis* 1973; **10**: 674–689.
11. Simpson A. On the solution of $S(\omega)X = 0$ by a Newtonian procedure. *Journal of Sound and Vibration* 1984; **97**: 153–164.
12. Sleijpen GLG, Booten AGL, Fokkema DR *et al*. Jacobi–Davidson type methods for generalized eigenproblems and polynomial eigenproblems. *BIT* 1996; **36**: 595–633.